AIMS Mathematics, 9(12): 34387–34405.
DOI:10.3934/math.20241638
Received: 14 August 2024
Revised: 11 November 2024
Accepted: 26 November 2024
Published: 06 December 2024

https://www.aimspress.com/journal/Math

Research article

Numerical solution of nonlinear complex integral equations using quasi-wavelets

Ahmed Ayad Khudhair, Saeed Sohrabi* and Hamid Ranjbar

Department of Mathematics, Faculty of Science, Urmia University, Urmia 57561-51818, Iran

* **Correspondence:** Email: s.sohrabi@urmia.ac.ir.

Abstract: In this paper, we introduced a numerical approach for estimating the solutions of nonlinear Fredholm integral equations in the complex plane. The main problem was transformed into a novel integral equation, which simplified the computation of integrals derived from the discretization technique. The combination of the standard collocation method with periodic quasi-wavelets, as well as their fundamental properties, was utilized to convert the solution of the newly formulated integral equation into a nonlinear complex system of algebraic equations. The convergence properties of the scheme were also presented. Finally, several numerical examples were provided to demonstrate the efficiency and precision of our proposed approach, which also confirmed its superiority over polynomial collocation methods.

Keywords: collocation method; Hammerstein integral equation; periodic quasi-wavelets; complex plane; convergence
Mathematics Subject Classification: 65N35, 65R20, 65T60

1. Introduction

Mathematical modeling of various physical problems, such as elasticity, fluid mechanics, and electromagnetic theory, typically leads to the formulation of different types of integral equations. Additionally, many boundary and initial value problems can be expressed as integral equations. Among these integral equations, the Fredholm linear equation and its nonlinear counterparts are frequently investigated due to their wide applications in signal processing, fluid mechanics, linear forward modeling, and inverse problems [28].

Our motivation in this paper is to consider the subsequent nonlinear integral equation

$$u(t) = f(t) + \int_0^{2\pi} k(t,s)g(s,u(s))ds, \quad t \in [0,2\pi], \tag{1.1}$$

where $u(t)$ is an unknown complex-valued function to be determined and f, k, and g are given continuous complex-valued periodic functions. The initial study of the real form of Eq (1.1) dates back to the 1920s when Hammerstein [12] considered the following boundary value problem:

$$u''(x) + f(x, u) = 0, \quad u(a) = 0, \quad u(b) = \beta,$$

and transformed it into a nonlinear integral equation. This resulting equation is commonly known as the Hammerstein integral equation. Equations of this type appear in many applications; for example, the nonlinear two-point boundary value problem [2]

$$u''(t) - \exp(u(t)) = 0, \ t \in [0, 1], \ u(0) = u(1) = 0,$$

which is evidently of some interest in magnetohydrodynamics and can be reformulated as the following nonlinear integral equation:

$$u(t) = \int_0^1 k(t, s) \exp(u(s)) ds, \quad t \in [0, 1],$$

where the kernel

$$k(t, s) = \begin{cases} -s(1 - t), & s \le t, \\ -t(1 - s), & s > t, \end{cases}$$

is the Green's function for the homogeneous problem $u''(t) = 0, \ t \in [0, 1], u(0) = u(1) = 0$.

Equation (1.1) is a particular case of the general form of the nonlinear integral equations

$$u(t) = f(t) + \int_a^b k(t, s, u(s)) ds, \quad t \in [a, b], \tag{1.2}$$

which has been initially introduced by Pavel Urysohn. The specific conditions concerning k and f under which a solution exists for the nonlinear Fredholm integral Eq (1.2) are [28]:

(i) The function $f(t)$ is bounded, $|f(t)| < R$, in $a \le t \le b$.

(ii) The function $k(t, s, u(s))$ is integrable and bounded where $|k(t, s, u(s))| < K$, in $a \le t, s \le b$.

(iii) The function $k(t, s, u(s))$ satisfies the Lipschitz condition

$$|k(t, s, z_1) - k(t, s, z_2)| < L|z_1 - z_2|.$$

Since then, several researchers have published papers that present numerical methods aimed at approximating real-type Hammerstein integral equations. The numerical treatment of both linear and nonlinear cases of (1.1) has been explored using various effective methods, such as projection methods [1, 14, 16], spline collocation [7, 17], Adomian's decomposition method [20], Sinc collocation [21], and wavelet-based methods [3, 19, 28]. For example, the generalized Burgers' (GB) equation has been solved using a time-space two-grid method [25]. The authors demonstrated that their proposed method offers several advantages over previous studies on the two-grid method, such as lower computational cost and simpler mesh selection. In [29], the orthogonal Gauss collocation method is introduced to approximate the solution of a two-dimensional (2D) fourth-order sub-diffusion

model. The researchers also analyzed the stability and super convergence properties of the method. Additionally, a new nonlinear finite-volume scheme, which preserves the discrete maximum principle (DMP), is used to solve the two-dimensional sub-diffusion equation on distorted meshes [30]. They showed that the proposed scheme is also applicable to distorted meshes without requiring stringent constraints. The general characteristic of these classical methods is that they are both efficient and effective for real-type integral equations. Furthermore, solving complex-type integral equations is significantly more challenging than solving their real counterparts. Consequently, only a few researchers have proposed numerical methods aimed at overcoming these difficulties [4, 5, 22].

On the other hand, the use of wavelet-based methods to solve integral equations is of significant interest. The first work was proposed by G. Beylkin et al. [6], in which the authors applied the Haar wavelet approach to solve an integral equation. Since then, many researchers have contributed to solving various types of integral equations using wavelets. Continuing this trend, researchers have introduced the concept of utilizing periodic quasi-wavelets, which trace their origins back to multi-resolution analysis and orthogonal periodic spline functions [13]. In theory, B-spline functions have been employed to generate periodic quasi-wavelets [8, 9, 13], with Han-Lin Chen [8, 9] being the first to explore integral equations through periodic quasi-wavelets. Furthermore, second-kind Fredholm integral equations can be accurately and easily solved in the complex plane by leveraging the rigorous properties of periodic quasi-wavelets. Therefore, the aim of this paper is to utilize periodic quasi-wavelets based on the collocation method for numerical solution of Eq (1.1). To do this, we start by converting Eq (1.1) into a new linear integral equation. This transformation simplifies the computation of integrals derived from the discretization technique and facilitates the process of solving the resulting system. Next, we approximate the solution of the new integral equation using functions that resemble the unknown function, which enhances the accuracy of our method. As a result, the accuracy of our numerical method approaches double precision, indicating that the error tends to zero.

The subsequent sections of the paper are structured in the following manner. A concise overview of the formulation of periodic quasi-wavelets is provided in Section 2. In Section 3, the standard collocation method based on periodic quasi-wavelets for solving Hammerstein integral equations is presented. The convergence rate of the method is studied in Section 4, and some numerical examples are given in Section 5 to verify the high accuracy and the wide applicability of the periodic quasi-wavelets method. Finally, some remarks conclude the paper in Section 6.

2. Construction of the periodic quasi-wavelets

The purpose of this section is to provide an overview of the basic formulation of the periodic quasi-wavelets in terms of B-spline functions [10, 11, 22].

Let

$$L_p^2[0,T] := \left\{ u : \int_0^T |u(t)|^2 dx < \infty,\ u(t) = u(t+T),\ \forall t \in \mathbb{R} \right\} \tag{2.1}$$

denote the set of all complex-valued periodic functions that are square integrable within the interval $[0, T]$ with a period of T where $T = hq$, in which h is a positive real number and $n, q \in \mathbb{N}$ so that $q \geq n + 1$. The related inner product over the above space is defined by

$$\langle u, v \rangle = \frac{1}{T} \int_0^T u(t)\overline{v(t)}dt. \tag{2.2}$$

Furthermore, assume that $h_m = \frac{T}{\kappa_m}$, where $\kappa_m = 2^m q$, $(m \in \mathbb{Z},\ m \geq 0)$. First, we introduce the periodic spline functions.

The periodic B-spline function $\mathcal{B}_p^{n,m}(t)$ of degree n with period T is defined by

$$\mathcal{B}_p^{n,m}(t) = (\kappa_m)^n \sum_{l\in\mathbb{Z}} \left(\frac{\sin(l\pi/\kappa_m)}{l\pi}\right)^{n+1} \exp\left(\frac{\mathrm{i}2\pi lt}{T}\right), \quad t \in \mathbb{R}, \tag{2.3}$$

where the related step size is h_m. The following aspects are considered by taking into account the main properties of spline functions (see [9, 23] for details):

(a) $\mathcal{V}_m \subset \mathcal{V}_{m+1},\ m \in \mathbb{Z}, m \geq 0$, where

$$\mathcal{V}_m = \mathrm{span}\Big\{\mathcal{B}_p^{n,m}(t - jh_m),\ j = 0, \ldots, \kappa_m - 1\Big\} \tag{2.4}$$

pertains to the set of periodic spline functions generated by the B-splines $\mathcal{B}_p^{n,m}(\cdot)$.

(b) $\overline{\bigcup_{m\in\mathbb{Z},m\geq 0} \mathcal{V}_m} = L_p^2[0, T]$, i.e., $\{\mathcal{V}_m\}$ is dense in $L_p^2[0, T]$.

(c) $\Big\{\mathcal{B}_p^{n,m}(t - jh_m),\ j = 0, \ldots, \kappa_m - 1\Big\}$ generates a base for $\mathcal{V}_m$.

It is easy to verify that $\mathcal{B}_p^{n,m}(t - jh_m),\ j = 0, \ldots, \kappa_m - 1$ forms a basis for $\mathcal{V}_m$. However, this basis is not orthogonal, which prompts us to construct an orthogonal basis for $\mathcal{V}_m$. To achieve this, we consider the functions $\mathcal{A}_\nu^{n,m}(t)$ defined as follows:

$$\mathcal{A}_\nu^{n,m}(t) = \eta_\nu^{n,m} \sum_{l=0}^{\kappa_m-1} \exp\Big(\frac{i2\pi l\nu}{\kappa_m}\Big)\mathcal{B}_p^{n,m}(t - lh_m), \quad t \in \mathbb{R}, \tag{2.5}$$

where

$$\eta_\nu^{n,m} = \Big\{x_0 + 2\sum_{\lambda=1}^{q} x_\lambda \cos(\lambda\nu h_m)\Big\}^{-1/2}, \quad x_\lambda = \mathcal{B}_p^{2q+1,m}(\lambda h_m). \tag{2.6}$$

To determine the properties of $\mathcal{A}_\nu^{n,m}(t)$, we need to calculate its Fourier series. Using Eqs (2.3) and (2.5), we can express the Fourier expansion of $\mathcal{A}_\nu^{n,m}(t)$ as follows:

$$\mathcal{A}_\nu^{n,m}(t) = \eta_\nu^{n,m}(\kappa_m)^{n+1} \sum_{\lambda\in\mathbb{Z}} \left(\frac{\sin(\nu\pi/(\kappa_m)}{(\nu + \lambda\kappa_m)\pi}\right)^{n+1} \exp\left(\frac{i2\pi(\nu + \lambda\kappa_m)t}{T}\right). \tag{2.7}$$

This representation leads to the following lemma and theorems:

Lemma 2.1 ([9]). *The set of functions $\{\mathcal{A}_\nu^{n,m}(t)\}_{\nu=0}^{\kappa_m-1}$ construct an orthonormal basis for $\mathcal{V}_m$, i.e.,*

$$\langle \mathcal{A}_{\nu_1}^{n,m}, \mathcal{A}_{\nu_2}^{n,m} \rangle = \delta_{\nu_1,\nu_2}, \quad \nu_1, \nu_2 = 0, \ldots, \kappa_m - 1, \tag{2.8}$$

where δ_{ν_1,ν_2} is the well-known Kronecker delta defined by

$$\delta_{\nu_1,\nu_2} = \begin{cases} 0, & \text{for } \nu_1 \neq \nu_2, \\ 1, & \text{for } \nu_1 = \nu_2. \end{cases}$$

Proof. By (2.3), we attain

$$\langle \mathcal{B}_l^{n,m}(\cdot), \mathcal{B}_k^{n,m}(\cdot)\rangle = (\kappa_m)^{-1}\mathcal{B}_p^{2n+1,m}((l-k)h_m), \tag{2.9}$$

where $\mathcal{B}_l^{n,m}$ is an extension of the B-spline functions defined in [9]. In this position, using (2.7) and (2.9), we get

$$\langle \mathcal{A}_{\nu_1}^{n,m}(\cdot), \mathcal{A}_{\nu_2}^{n,m}(\cdot)\rangle = \left(\eta_{\nu_1}^{n,m}\right)^2 \delta_{\nu_1,\nu_2} \sum_{l=0}^{\kappa_m-1} \exp\left(\frac{\mathrm{i}2\pi l\nu_2}{\kappa_m}\right)\mathcal{B}_p^{2n+1}(lh_m, h_m), \tag{2.10}$$

where $\mathcal{B}_p^{2n+1}(\cdot, h_m) := \mathcal{B}_p^{2n+1,m}(\cdot)$. Then according to properties of B-spline functions, we have [9]

$$\mathcal{B}_p^{2n+1}(ah_m, h_m) = \mathcal{B}_p^{2n+1}(ah, h),$$

and

$$\mathcal{B}_p^{2n+1}(-ah, h) = \mathcal{B}_p^{2n+1}(ah, h) = \mathcal{B}_p^{2n+1}(a, 1).$$

Define

$$\begin{aligned} E(n,\nu,m) :&= \sum_{l=0}^{\kappa_m-1} \exp\Big(\frac{\mathrm{i}2\pi l\nu}{\kappa_m}\Big)\mathcal{B}_p^{2n+1}(lh_m, h_m) \\ &= \sum_{l=0}^{n} \exp\Big(\frac{\mathrm{i}2\pi\nu lh_m}{T}\Big)\mathcal{B}_p^{2n+1}(l,1) + \sum_{l=1}^{n} \exp\Big(\frac{\mathrm{i}2\pi\nu(-l)h_m}{T}\Big)\mathcal{B}_p^{2n+1}(l,1) \\ &= \mathcal{B}_p^{2n+1}(0,1) + 2\sum_{l=1}^{n} \cos\Big(\frac{\mathrm{i}2\pi\nu lh_m}{T}\Big)\mathcal{B}_p^{2n+1}(l,1) \\ &= x_0 + 2\sum_{l=1}^{n} \cos\Big(\frac{\mathrm{i}2\pi\nu lh_m}{T}\Big)x_l = \left(\eta_{\nu_1}^{n,m}\right)^{-2}. \end{aligned} \tag{2.11}$$

Therefore, $E(n,\nu,m)\left(\eta_{\nu_1}^{n,m}\right)^2 = 1$, and by Eq (2.10), we have

$$\langle \mathcal{A}_{\nu_1}^{n,m}(\cdot), \mathcal{A}_{\nu_2}^{n,m}(\cdot)\rangle = \delta_{\nu_1,\nu_2}, \quad \text{for } 0 \le \nu_1, \nu_2 \le \kappa_m - 1.$$

□

In the following theorem, we provide an alternative representation of the refinable equation associated with $\mathcal{A}_\nu^{n,m}(t)$. This form highlights the fundamental characteristics of this function.

Theorem 2.1. *The function $\mathcal{A}_\nu^{n,m}$ has the following two-scale representation:*

$$\mathcal{A}_\nu^{n,m} = a_\nu^{n,m+1}\mathcal{A}_\nu^{n,m+1} + b_\nu^{n,m+1}\mathcal{A}_{\nu+\kappa_m}^{n,m+1}, \tag{2.12}$$

where the constants $a_\nu^{n,m+1}$ and $b_\nu^{n,m+1}$ are given by

$$a_\nu^{n,m+1} = \frac{\eta_\nu^{n,m}}{\eta_\nu^{n,m+1}}\Big(\cos\frac{\nu\pi}{\kappa_{m+1}}\Big)^{n+1}, \tag{2.13}$$

$$b_\nu^{n,m+1} = \frac{\eta_\nu^{n,m}}{\eta_{\nu+\kappa_m}^{n,m+1}}\Big(\sin\frac{\nu\pi}{\kappa_{m+1}}\Big)^{n+1}, \tag{2.14}$$

$\nu = 0, \ldots, \kappa_m - 1$, and $\eta_\nu^{n,m}$ is given as in (2.6).

Proof. See [9]. □

Now, we introduce functions $\mathcal{D}_\nu^{n,m}(t)$, corresponding to $\mathcal{A}_\nu^{n,m}$, as

$$\mathcal{D}_\nu^{n,m}(t) := b_\nu^{n,m+1}\mathcal{D}_\nu^{n,m+1}(t) - a_\nu^{n,m+1}\mathcal{D}_{\nu+\kappa_m}^{n,m+1}(t), \quad \nu = 0, \ldots, \kappa_m - 1, \quad t \in \mathbb{R}, \tag{2.15}$$

and prove that they are the wavelet functions. Initially, we recall the following properties of these functions:

(i) $\langle \mathcal{D}_{\nu_1}^{n,m}, \mathcal{D}_{\nu_2}^{n,m} \rangle = \delta_{\nu_1,\nu_2}, \quad \nu_1, \nu_2 = 0, \ldots, \kappa_m - 1,$

(ii) $\mathcal{D}_\nu^{n,m} \in \mathcal{V}_{m+1}, \quad 0 \le \nu \le \kappa_m - 1,$

(iii) $\langle \mathcal{D}_{\nu_1}^{n,m}, \mathcal{A}_{\nu_2}^{n,m} \rangle = 0, \quad 0 \le \nu_1, \nu_2 \le \kappa_m - 1.$

These properties lead to the following theorem.

Theorem 2.2. *The functions* $\{\mathcal{D}_\nu^{n,m}(t)\}_{\nu=0}^{\kappa_m-1}$ *generate a basis set for* $\mathcal{W}_m$*, which is orthonormal and* $\mathcal{V}_{m+1} = \mathcal{V}_m \oplus \mathcal{W}_m$*, where*

$$\mathcal{W}_m = \text{span}\Big\{\mathcal{D}_\nu^{n,m} \Big|\ \nu = 0, \ldots, \kappa_m - 1\Big\}. \tag{2.16}$$

Proof. The proof is given in [9]. □

The functions $\mathcal{A}_\nu^{n,m}$ and $\mathcal{D}_\nu^{n,m}$ are commonly referred to as the father and mother quasi-wavelets, respectively. It is important to mention that using the word "quasi" before the term "wavelet" implies a distinction between them in the concept of Meyer.

Proposition 2.1. *Assume that* $P_m u(t) = \sum_{l=0}^{\kappa_m-1} \langle u, \mathcal{A}_l^{n,m} \rangle \mathcal{A}_l^{n,m}(t)$*. Then, the following statements hold for any* $u \in L_p^2[0, T]$*:*

(1) $\|P_m\|_2 \le 1,$

(2) $\lim_{m\to\infty} \|u - P_m u\|_2 = 0.$

Proof. (1) Let $Q_m u(t) = \sum_{l=0}^{\kappa_m-1} \langle u, \mathcal{D}_l^{n,m} \rangle \mathcal{D}_l^{n,m}(t)$. It follows from (b) and Theorem 2.2 that

$$u(t) = P_m u(t) + \sum_{m' \ge m} Q_{m'} u(t).$$

Hence,

$$\|u\|^2 = \langle u, u \rangle = \langle P_m u + \sum_{m' \ge m} Q_{m'} u, P_m u + \sum_{m' \ge m} Q_{m'} u \rangle = \langle P_m u, P_m u \rangle + \langle \sum_{m' \ge m} Q_{m'} u, \sum_{m' \ge m} Q_{m'} u \rangle \ge \|P_m u\|^2,$$

which indicates that $\|P_m\| \le 1$.
(2) Fix u and choose any $\epsilon > 0$. From conditions (a) and (b), since $\{\mathcal{V}_m\}$ is dense in $L_p^2[0, T]$, we can find an $n \in \mathbb{N}$ and a function $g \in \mathcal{V}_n$ so that $\|u - g\| < \epsilon$. In fact, g is automatically in $\mathcal{V}_m$ for all $m \ge n$; $P_n u$ is the closest function in $\mathcal{V}_n$ to u, so that

$$\|u - P_m u\| \le \|u - g\| < \epsilon, \quad \text{for all } m \ge n.$$

□

For the 2-dimensional case, the above methodology can be used to obtain a basis for $L_p^2([0, T]^2)$ by the tensor product.

3. Discretization of nonlinear integral equations

The aim of this section is to introduce a collocation method based on periodic quasi-wavelets for solving Eq (1.1). Instead of applying the collocation approach to the original form of Eq (1.1), we use the method to approximate the solution of an equivalent form of the equation. More precisely, we first assume

$$v(t) := g(t, u(t)), \quad t \in [0, 2\pi]. \tag{3.1}$$

By substituting (3.1) into (1.1), we get

$$u(t) = f(t) + \int_0^{2\pi} k(t, s)v(s)ds, \quad t \in [0, 2\pi], \tag{3.2}$$

which results that the new unknown function $v(t)$ satisfies the following nonlinear integral equation:

$$v(t) = g\left(t, f(t) + \int_0^{2\pi} k(t, s)v(s)ds\right), \quad t \in [0, 2\pi]. \tag{3.3}$$

Now, we use periodic quasi-wavelets constructed on $[0, 2\pi]$ (provided in Section 2) to approximate the kernel function, and then get the numerical solutions using the degenerate kernel procedure combined with the classical collocation method.

Suppose that $\{\mathcal{A}_j^{n,m}\}$ are the periodic quasi-wavelets described in Section 2. Then, the kernel function $k(t, s)$ can be evaluated by a degenerate combination as

$$k_m(t, s) = \sum_{i,j=0}^{\kappa_m-1} \alpha_{ij}^m \mathcal{A}_i^{n,m}(t)\mathcal{A}_j^{n,m}(s), \tag{3.4}$$

where α_{ij}^m are provided by

$$\alpha_{ij}^m = \langle \mathcal{A}_i^{n,m}(t), \langle k(t, s), \mathcal{A}_j^{n,m}(s)\rangle\rangle. \tag{3.5}$$

Also, we can approximate $v(t)$ in terms of a linear combination of periodic quasi-wavelets as

$$v_m(t) = \sum_{l=0}^{\kappa_m-1} a_l^m \mathcal{A}_l^{n,m}(t), \qquad t \in [0, 2\pi], \tag{3.6}$$

where a_l^m are unknown coefficients that need to be determined based on certain conditions. Substituting (3.4) and (3.6) into (3.3) and using the orthonormality property of $\{\mathcal{A}_l^{n,m}; 0 \le l \le \kappa_m - 1\}$, we find that

$$\sum_{l=0}^{\kappa_m-1} a_l^m \mathcal{A}_l^{n,m}(t) = g\left(t, f(t) + \sum_{i,j=0}^{\kappa_m-1} a_j^m \alpha_{ij}^m \mathcal{A}_i^{n,m}(t)\right), \tag{3.7}$$

where the coefficients $a_l^m,\ 0 \le l \le \kappa_m - 1$ are evaluated by the κ_m collocation conditions

$$\sum_{l=0}^{\kappa_m-1} a_l^m \mathcal{A}_l^{n,m}(\tau_i^m) = g\left(\tau_i^m, f(\tau_i^m) + \sum_{i,j=0}^{\kappa_m-1} a_j^m \alpha_{ij}^m \mathcal{A}_i^{n,m}(\tau_i^m)\right), \quad 0 \le i \le \kappa_m - 1, \tag{3.8}$$

where τ_i^m are distinct points in $[0, 2\pi]$.

Equation (3.8) leads to a nonlinear system consisting of κ_m algebraic equations for a_l^m, which can be solved using an appropriate iterative method. Finally, by substituting the approximation v_m into the righthand side of Eq (3.2), we obtain the estimated solution $u_m(t)$ for our Hammerstein integral Eq (1.1). This means that the approximate solution u_m can be resulted by

$$u_m(t) := f(t) + \int_0^{2\pi} k(t,s)v_m(s)ds. \tag{3.9}$$

4. Convergence analysis

This section is dedicated to derive suitable assumptions in which, under these conditions the approximation v_m converges to an exact solution of (3.3). Our intention is to analyze the convergence attributes of the suggested numerical method through the application of the ideas discussed in [24, 27].

Let us assume that there is some ball $B(u^*, \delta) = \{u \in L_p^2[0,T] : \|u - u^*\| \leq \delta\}$, $\delta > 0$, such that it contains only the solution $u^*(t)$ of Eq (1.1) which is to be determined, that is, the solution u^* is geometrically isolated [15]. For convenience of presentation, we define the following operators:

$$\begin{aligned}
&(\mathcal{K}u)(t) := \int_0^{2\pi} k(t,s)u(s)ds, \quad (\mathcal{K}_m u)(t) := \int_0^{2\pi} k_m(t,s)u(s)ds,\\
&\mathcal{T}(u)(t) := f(t) + (\mathcal{K}u)(t), \quad \mathcal{T}_m(u)(t) := f(t) + (\mathcal{K}_m u)(t),\\
&\mathcal{G}(u)(t) := g(t, u(t)).
\end{aligned}$$

With the above notations, Eqs (1.1), (3.3), and (3.8) can be written more compactly as

$$u = \mathcal{T}\mathcal{G}(u), \quad u \in L_p^2[0,T], \tag{4.1}$$

$$v = \mathcal{G}\mathcal{T}(v), \quad v \in L_p^2[0,T], \tag{4.2}$$

$$v_m = P_m\mathcal{G}\mathcal{T}_m(v_m), \quad v_m \in \mathcal{V}_m. \tag{4.3}$$

Before providing the methodology of the convergence phenomenon, we first make some assumptions which are usually essential to derive the convergence results:

A1. $f \in L_p^2[0,T]$.

A2. The kernel function $k \in L_p^2([0,T]^2)$, and satisfies

$$\lim_{t \to t'} \int_0^{2\pi} |k(t,s) - k(t',s)|^2 ds = 0, \quad t' \in [0, 2\pi].$$

A3. The function $g(t,u)$ is continuous on $[0,2\pi] \times \mathbb{C}$ and Lipschitz continuous with respect to u, i.e., $|g(t,u_1) - g(t,u_2)| \leq C_1|u_1 - u_2|$ for some constant $C_1 > 0$, $t \in [0,2\pi]$, and all $u_1, u_2 \in B(u^*, \delta)$.

A4. The partial derivative $g^{(0,1)}(t,u) := (\partial/\partial u)g(t,u)$ is a continuous function on $[0,2\pi]$ with respect to t and is Lipschitz continuous with respect to u around u^*.

A5. The Fréchet derivative of the operator $\mathcal{G}\mathcal{T}$ has a regular value of 1 at the point v^*, i.e., the inverse $(I - (\mathcal{G}\mathcal{T})'(v^*))^{-1}$ exists and is a bounded linear operator.

A6. $v^* \in L_p^2[0, T]$ is a unique local solution for Eq (4.3).

In the remaining of this part, we attempt to obtain the convergence property of the suggested scheme step-by-step.

Step 1. In this step, we demonstrate that the convergence rate of u_m to u^* is strongly dependent on the convergence rate of v_m to v^*.

Proposition 4.1.

$$\|u^* - u_m\| \leq M \, \|v^* - v_m\|, \tag{4.4}$$

where

$$M = \left(\int_0^{2\pi} \int_0^{2\pi} |k(t, s)|^2 ds dt \right)^{1/2} < \infty.$$

Proof. Given the definitions of u^* and u_m, we obtain

$$u^*(t) = f(t) + \int_0^{2\pi} k(t, s) v^*(s) ds, \quad t \in [0, 2\pi],$$

and

$$u_m(t) = f(t) + \int_0^{2\pi} k(t, s) v_m(s) ds, \quad t \in [0, 2\pi].$$

With the above equations, we get

$$u^*(t) - u_m(t) = \int_0^{2\pi} k(t, s)(v^*(s) - v_m(s)) ds, \quad t \in [0, 2\pi].$$

Therefore, we have

$$\|u^*(t) - u_m(t)\| = \left\| \int_0^{2\pi} k(t, s)(v^*(s) - v_m(s)) ds \right\| = \|\mathcal{K}(v^* - v_m)\|, \quad t \in [0, 2\pi]. \tag{4.5}$$

Finally, by using the Cauchy-Schwarz inequality, we obtain

$$\begin{aligned} \|\mathcal{K}(v^* - v_m)\|^2 &= \int_0^{2\pi} \left| \int_0^{2\pi} k(t, s)(v^* - v_m)(s) ds \right|^2 dt \\ &\leq \int_0^{2\pi} \left(\int_0^{2\pi} |k(t, s)|^2 ds \right) \left(\int_0^{2\pi} \left| (v^* - v_m)(s) \right|^2 ds \right) dt \\ &= M^2 \|v^* - v_m\|^2, \end{aligned}$$

or

$$\|u^* - u_m\| \leq M \, \|v^* - v_m\|, \tag{4.6}$$

and the proof is complete. □

The above proposition implies that the rate of convergence of u_m to u^* is determined by the rate of convergence of v_m to v^*.

Step 2. In this position, we demonstrate that v^* converges to v, and we also derive an error bound for the method presented.

Lemma 4.1. *Suppose that the assumptions A1 to A6 hold. Then, for a sufficiently large m, $I-(P_m\mathcal{G}\mathcal{T}_m)'(v^*)$ is invertible and $[I-(P_m\mathcal{G}\mathcal{T}_m)'(v^*)]^{-1}$ is uniformly bounded, where the projection operators P_m and Q_m are defined as in Proposition 2.1.*

Proof. According to assumption A3, the inverse of $(I-(\mathcal{G}\mathcal{T})'(v^*))$ exists and, thus,

$$\Big(I-(P_m\mathcal{G}\mathcal{T}_m)'(v^*)\Big)\Big(I-(\mathcal{G}\mathcal{T})'(v^*)\Big)^{-1}=I+\Big((\mathcal{G}\mathcal{T})'(v^*)-(P_m\mathcal{G}\mathcal{T}_m)'(v^*)\Big)\Big(I-(\mathcal{G}\mathcal{T})'(v^*)\Big)^{-1}. \tag{4.7}$$

Since

$$\|\mathcal{K}-\mathcal{K}_m\|\overset{m\to\infty}{\longrightarrow}0,\quad \|I-P_m\|\overset{m\to\infty}{\longrightarrow}0,$$

we thus deduce that for a sufficiently large m,

$$\begin{aligned}
&\|((\mathcal{G}\mathcal{T})'(v^*)-(P_m\mathcal{G}\mathcal{T}_m)'(v^*))(I-(\mathcal{G}\mathcal{T})'(v^*))^{-1}\|\\
&=\|((\mathcal{G}\mathcal{T})'(v^*)-(P_m\mathcal{G}\mathcal{T})'(v^*)+(P_m\mathcal{G}\mathcal{T})'(v^*)-(P_m\mathcal{G}\mathcal{T}_m)'(v^*))(I-(\mathcal{G}\mathcal{T})'(v^*))^{-1}\|\\
&=(\|I-P_m\|.\|(\mathcal{G}\mathcal{T})'(v^*)\|+\|\mathcal{G}'(\mathcal{T}v^*).\mathcal{T}v^*-\mathcal{G}'(\mathcal{T}_mv^*).\mathcal{T}_mv^*\|).\|(I-(\mathcal{G}\mathcal{T})'(v^*))^{-1}\|\\
&\le C_2\|I-P_m\|+C_3\|\mathcal{G}'(\mathcal{T}v^*).\mathcal{T}v^*-\mathcal{G}'(\mathcal{T}v^*).T_mv^*+\mathcal{G}'(\mathcal{T}v^*).\mathcal{T}_mv^*-\mathcal{G}'(\mathcal{T}_mv^*).\mathcal{T}_mv^*\|\\
&\le C_4\|I-P_m\|+C_5\|\mathcal{K}-\mathcal{K}_m\|\\
&\le\frac{1}{2}.
\end{aligned}$$

This implies that for a sufficiently large m, the operator

$$I+((\mathcal{G}\mathcal{T})'(v^*)-(P_m\mathcal{G}\mathcal{T}_m)'(v^*))(I-(\mathcal{G}\mathcal{T})'(v^*))^{-1}$$

is invertible, and, therefore, for all such m we have

$$\Big(I+((\mathcal{G}\mathcal{T})'(v^*)-(P_m\mathcal{G}\mathcal{T}_m)'(v^*))(I-(\mathcal{G}\mathcal{T})'(v^*))^{-1}\Big)^{-1}\le C_6,$$

for some constant C_6. This inequality, together with (4.7), implies that for a sufficiently large m, $I-(P_m\mathcal{G}\mathcal{T}_m)'(v^*)$ is invertible and then

$$\begin{aligned}
&\|(I-(P_m\mathcal{G}\mathcal{T}_m)'(v^*))^{-1}\|\\
&=\|(I-(\mathcal{G}\mathcal{T})'(v^*))^{-1}.\Big(I+((\mathcal{G}\mathcal{T})'(v^*)-(P_m\mathcal{G}\mathcal{T}_m)'(v^*))(I-(\mathcal{G}\mathcal{T})'(v^*))^{-1}\Big)^{-1}\|\\
&\le C_6\|(I-(\mathcal{G}\mathcal{T})'(v^*))^{-1}\|.
\end{aligned}$$

This completes the proof of Lemma 4.1. □

The above lemma allows us to obtain the convergence rate of v_m for an exact solution of (4.3).

Theorem 4.1. *Let the assumptions of Lemma 4.1 hold. Then, there exists a neighborhood of v^* so that for sufficiently large m, there exists a unique approximation v_m defined by the unique solution of the linear algebraic complex systems* (4.3) *and the periodic quasi-wavelets representations* (3.8)*. Moreover, we have the estimate*

$$\|v^*-v_m\|\le\alpha\|v^*-P_mv^*\|+\beta\|(\mathcal{K}-\mathcal{K}_m)v^*\|, \tag{4.8}$$

where α,β are independent of m.

Proof. Let

$$B(v^*, \delta) = \{v \in L_p^2[0,T] : \|v - v^*\| \leq \delta\},$$

be a neighborhood of v^* where $\delta < 1/(C_1C_6\|(I - (\mathcal{GT})'(v^*))^{-1}\|.\|k\|_{L_p^2[0,T]})$. Assuming

$$\mathcal{U}_m = v^* + (I - (P_m\mathcal{GT}_m)'(v^*))^{-1}\Big(P_m\mathcal{GT}_m v - \mathcal{GT}v^* - (P_m\mathcal{GT}_m)'(v^*)(v - v^*)\Big),$$

and using the Lipschitz continuity of $g^{(0,1)}$, it is apparent that $\mathcal{U}_m$ acts as a contraction mapping over the ball $B(z^*, \delta)$, provided that m is sufficiently large [24]. This together with the contraction mapping theorem implies that for any u in the ball $B(v^*, \delta)$, the operator equation $u = \mathcal{U}_m u$ has a unique solution u_m for a sufficiently large m. Hence, Eq (4.3) has a local unique solution.

In order to obtain the estimate (4.8), using $v^* = \mathcal{GT}(v^*)$ and $v_m = P_m\mathcal{GT}_m(v_m)$, we get

$$\begin{aligned} v^* - v_m &= v^* - P_m v^* + P_m\mathcal{GT}(v^*) - P_m\mathcal{GT}_m(v^*) + P_m\mathcal{GT}_m(v^*) - P_m\mathcal{GT}_m(v_m) \\ &= (I - (P_m\mathcal{GT}_m)'(v^*))^{-1}\Big(v^* - P_m v^* + P_m\mathcal{GT}(v^*) - P_m\mathcal{GT}_m(v^*) + \omega_m\Big), \end{aligned}$$

where $\omega_m = P_m\mathcal{GT}_m(v^*) - P_m\mathcal{GT}_m(v_m) - (P_m\mathcal{GT}_m)'(v^*)(v^* - v_m)$. Therefore, it follows from Proposition 2.1, assumption A3, and Lemma 4.1 that

$$\begin{aligned} \|v^* - v_m\| &\leq C_7\|v^* - P_m v^* + P_m\mathcal{GT}(v^*) - P_m\mathcal{GT}_m(v^*) + \omega_m\| \\ &\leq C_7\Big(\|v^* - P_m v^*\| + \|P_m\mathcal{GT}(v^*) - P_m\mathcal{GT}_m(v^*)\| + \|\omega_m\|\Big) \\ &\leq C_7\|v^* - P_m v^*\| + C_8\|\mathcal{T}(v^*) - \mathcal{T}_m(v^*)\| + C_7\|\omega_m\| \\ &= C_7\|v^* - P_m v^*\| + C_9\|(\mathcal{K} - \mathcal{K}_m)(v^*)\| + C_7\|\omega_m\|. \end{aligned}$$

To complete the proof, we need to show that $\|\omega_m\| = O(\|v^* - v_m\|)$. For this purpose, by Proposition 2.1, we have

$$\begin{aligned} \|\omega_m\| &= \|P_m\mathcal{GT}_m(v^*) - P_m\mathcal{GT}_m(v_m) - (P_m\mathcal{GT}_m)'(v^*)(v^* - v_m)\| \\ &\leq \|\mathcal{GT}_m(v^*) - \mathcal{GT}_m(v_m) - (\mathcal{GT}_m)'(v^*)(v^* - v_m)\| \\ &= \Big\|\big[(\mathcal{GT}_m)'(v^* + \alpha\Delta v) - (\mathcal{GT}_m)'(v^*)\big](v^* - v_m)\Big\|, \;\; 0 < \alpha < 1, \; \Delta v := v^* - v_m \\ &\leq C_{10}\,\|\mathcal{T}_m(v^*) - \mathcal{T}_m(v_m)\| \cdot \|\Delta v\| \\ &= C_{10}\,\|\mathcal{K}_m(v^*) - \mathcal{K}_m(v_m)\| \cdot \|\Delta v\| \\ &= C_{10}\,\|\mathcal{K}_m\Delta v\| \cdot \|\Delta v\| \\ &\leq C_{10}\,\|\mathcal{K}_m\|_{L_p^2([0,T])^2} \cdot \|\Delta v\|^2 \\ &= O(\|v^* - v_m\|) \; (m \to \infty). \end{aligned}$$

□

Corollary 4.1. *Suppose that $v^* \in H^s[0, 2\pi]$, and r is the Holder index of the functions $\mathcal{A}^{n,m}, \mathcal{D}^{n,m}$ defined in Section 2. Then, with the L^2-norm, we have*

$$\|v^* - v_m\| = O(2^{-ms}), \tag{4.9}$$

where $s < r$.

Proof. By the definitions of P_m and Q_m in Proposition 2.1, we have

$$\begin{aligned}\|v^* - P_m v^*\|^2 &= \left\| \sum_{m' \geq m} Q_{m'} v^* \right\|^2 = \left\| \sum_{m' \geq m} \sum_{l=0}^{\kappa_{m'}-1} \langle v^*, \mathcal{D}_l^{n,m'} \rangle \mathcal{D}_l^{n,m'} v^* \right\|^2 = \sum_{m' \geq m} \sum_{l=0}^{\kappa_{m'}-1} \left| \langle v^*, \mathcal{D}_l^{n,m'} \rangle \right|^2 \\ &\leq \sum_{m' \geq m} \sum_{l=0}^{\kappa_{m'}-1} \left(C_{11} 2^{-m'(s+1/2)} \right)^2 = \sum_{m' \geq m} C_{12} 2^{m'} . 2^{-2m's - m'} = \sum_{m' \geq m} C_{12} 2^{-2m's} \\ &< C_{13} 2^{-2ms}.\end{aligned}$$

Therefore, $\|v^* - P_m v^*\| \leq C_{14} 2^{-ms}$. In a similar manner, we have $\|(\mathcal{K} - \mathcal{K}_m) v^*\| \leq C_{15} 2^{-ms}$. Then, the proof is completed by appealing Theorem 4.1. □

At the conclusion of this section, it is important to highlight that all results obtained earlier are still applicable within the context of the following norm:

$$\|f\|_C = \max_{0 \leq t \leq 2\pi} |f(t)|, \quad \forall f \in C[0, 2\pi],$$

and one can easily show that

$$\|u^* - u_m\|_C \leq M \|v^* - v_m\|_C,$$

where

$$M = \max_{0 \leq t \leq 2\pi} \int_0^{2\pi} |k(t, s)| ds.$$

5. Numerical examples

In this section, we numerically solve some nonlinear integral equations by our new method in which the basis functions

$$\{\mathcal{A}_i^{n,m}\}, \quad i = 0, \ldots, \kappa_m - 1$$

are taken as periodic quasi-wavelets where n denotes the degree of quasi-wavelets. We choose τ_i^m as collocation points where they belong to the following uniform grid

$$I = \left\{ \tau_i^m : \ \tau_i^m = \frac{2\pi}{\kappa_m - 1} i, \quad i = 0, \ldots, \kappa_m - 1 \right\}.$$

To demonstrate the efficiency and accuracy of the proposed method, we compute the difference between the numerical and exact solution of the underlying problem at the following equidistant points

$$t_i = \frac{2\pi}{9} i, \quad i = 0, \ldots, 9,$$

and outline absolute errors (AEs) by employing established results. Moreover, we display the numerical and exact solutions for each example, and graph the AEs in a logarithmic scale for different values of m and n to validate the theoretical findings. It is important to mention that there are no limitations on selecting the value of n, which can be any positive integer. However, selecting the value of m requires practical expertise and should be carried out in a manner that facilitates the solution of the resulting system of nonlinear algebraic equations as effortlessly as possible. The implementation of all numerical computations was carried out using Mathematica software on a common PC computer.

Example 5.1. *As the first example, take into account the subsequent nonlinear complex integral equation*

$$u(t) = f(t) + i \int_0^{2\pi} \frac{\sin(s)}{\sqrt[3]{e^{1+\sin(t)}}} u^2(s) ds, \tag{5.1}$$

where $f(t)$ is determined in such a way that it yields the exact solution $u(t) = 5\cos(t) + 2\sin(5t) + i(5\sin(t) + 2\cos(5t))$. We solve this integral equation by our method with the periodic quasi-wavelets of order $n = 2$ and list the AEs at points t_i, $i = 0, \ldots, 9$ for $m = 1, 2$ in Table 1. Figure 1 illustrates the errors detailed in Table 1 using a logarithmic scale. Table 1 as well as Figure 1 indicates that the AEs at points t_i decay rapidly as m increases. In order to demonstrate the high accuracy of the proposed method, the comparison between the analytic and approximate solutions for $m = 1, 2$ are shown in Figure 2. Figure 2 confirms that the proposed scheme gives almost the same solution as the analytic method.

Table 1. The AEs at points t_i, $i = 0, \ldots, 9$ for $m = 1, 2$ in Example 5.1.

t_i	$m = 1$	$m = 2$
$t_0 = 0$	3.32029×10^{-01}	4.96507×10^{-15}
$t_1 = \frac{2\pi}{9}$	2.67993×10^{-01}	4.31133×10^{-15}
$t_2 = \frac{4\pi}{9}$	2.39117×10^{-01}	4.09430×10^{-15}
$\vdots$	$\vdots$	$\vdots$
$t_7 = \frac{14\pi}{9}$	4.61043×10^{-01}	3.55271×10^{-15}
$t_8 = \frac{16\pi}{9}$	4.11366×10^{-01}	4.09430×10^{-15}
$t_9 = 2\pi$	3.32029×10^{-01}	4.57353×10^{-15}

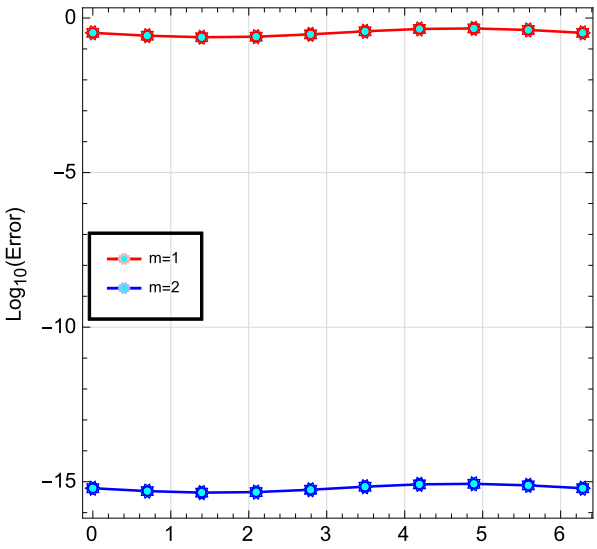

Figure 1. The logarithmic error associated with the proposed method in Example 5.1 with $m = 1, 2$.

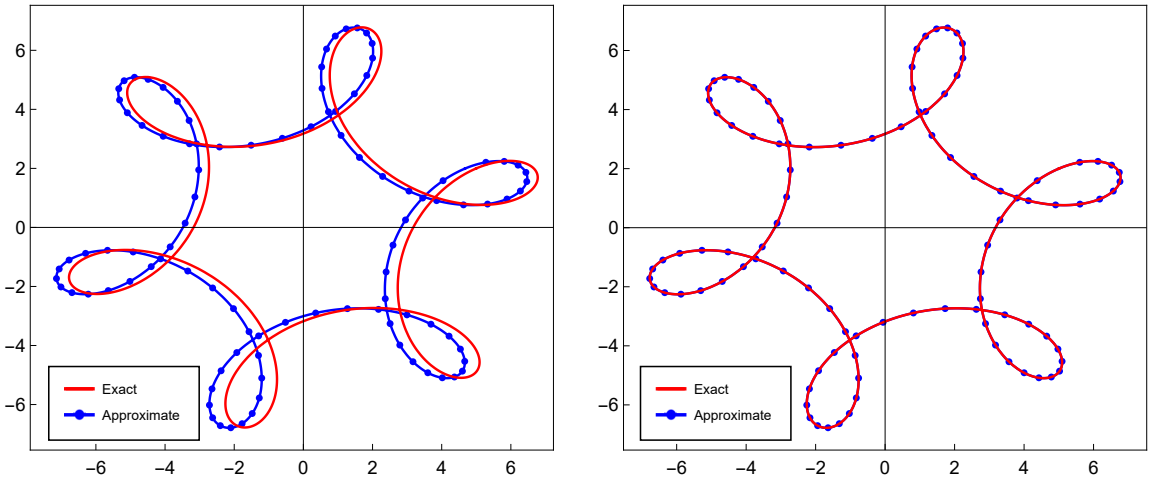

Figure 2. Parametric plot of the approximate and exact solutions for $m = 1$ (left) and $m = 2$ (right) in Example 5.1.

Example 5.2. *As the second example, consider the following complex integral equation:*

$$u(t) = \frac{67}{40}\cos^3(t) + i\sin^3(t) + \frac{8}{5\pi i}\int_0^{2\pi} \cos^3(t)\sin^3(s)u^3(s)ds. \tag{5.2}$$

It is straightforward to confirm that the analytical solution for this integral equation is $u(t) = \cos^3(t) + i\sin^3(t)$. *Similar to the previous example, we solve the above equation with the periodic quasi-wavelets of order* $n = 2$, *obtain the AEs at points* $t_i,\ i = 0, \ldots, 9$ *for* $m = 1, 2$, *and report them in Table 2. The experimental results indicate that better approximation is expected by choosing* $m = 2$, *which we get*

$$\|u^* - u_m\| = 4.58300 \times 10^{-17}.$$

Table 2. The AEs at points $t_i,\ i = 0, \ldots, 9$ for $m = 1, 2$ in Example 5.2.

t_i	$m = 1$	$m = 2$
$t_0 = 0$	1.90067×10^{-02}	4.58300×10^{-17}
$t_1 = \frac{2\pi}{9}$	8.54413×10^{-03}	3.87800×10^{-17}
$t_2 = \frac{4\pi}{9}$	9.95214×10^{-05}	2.25200×10^{-17}
$\vdots$	$\vdots$	$\vdots$
$t_7 = \frac{14\pi}{9}$	9.95214×10^{-05}	2.25200×10^{-17}
$t_8 = \frac{16\pi}{9}$	8.54413×10^{-03}	3.87800×10^{-17}
$t_9 = 2\pi$	1.90067×10^{-02}	4.58300×10^{-17}

To demonstrate the exceptional accuracy of the proposed method, we present a logarithmic scale representation of the resulting errors for $m = 1, 2$ *in Figure 3. We also compare the analytic and approximation solutions for* $m = 1, 2$ *in Figure 4. Figure 4 again shows the high accuracy of the proposed scheme and verifies theoretical results.*

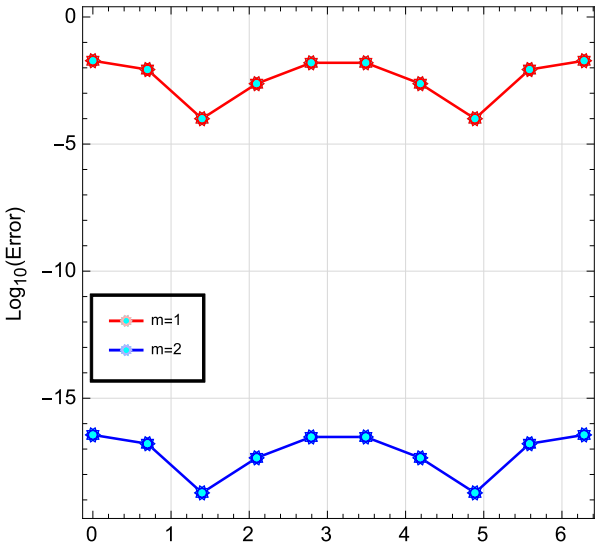

Figure 3. The logarithmic error associated with the proposed method for Example 5.2 with $m = 1, 2$.

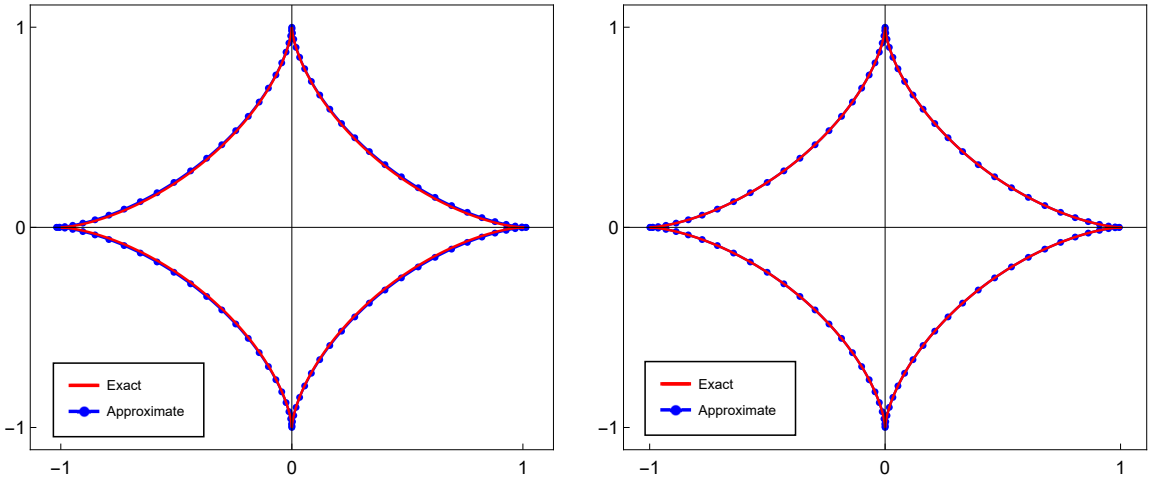

Figure 4. Parametric plot of the approximate and exact solutions for $m = 1$ (left) and $m = 2$ (right) in Example 5.2.

Example 5.3. *As the final example, consider the following nonlinear integral equation:*

$$u(t) = (1 - \frac{3\pi}{4})\sin(t) + \int_0^{2\pi} \cos(t - s)u^3(s)ds. \tag{5.3}$$

One can readily verify that the analytical solution to this integral equation is $u(t) = \sin(t)$. *In a manner consistent with the earlier examples, we calculate the AEs at the specified points* t_i, $i = 0, \ldots, 9$ *for* $m = 1, 2$, *and present the results in Table 3. In addition, Figure 5 provides a graphical depiction of the results contained in Table 3. The numerical results consistently reveal that the error of the proposed approach decreases as m increases, which supports the theoretical findings.*

Table 3. The AEs at points $t_i,\ i = 0, \ldots, 9$ for $m = 1, 2$ in Example 5.3.

t_i	$m = 1$	$m = 2$
$t_0 = 0$	3.42082×10^{-03}	9.66200×10^{-16}
$t_1 = \frac{2\pi}{9}$	1.02350×10^{-04}	9.74700×10^{-16}
$t_2 = \frac{4\pi}{9}$	1.56809×10^{-04}	9.96400×10^{-16}
$\vdots$	$\vdots$	$\vdots$
$t_7 = \frac{14\pi}{9}$	1.56809×10^{-04}	1.00900×10^{-15}
$t_8 = \frac{16\pi}{9}$	1.02350×10^{-04}	9.84000×10^{-16}
$t_9 = 2\pi$	3.42082×10^{-03}	9.68000×10^{-16}

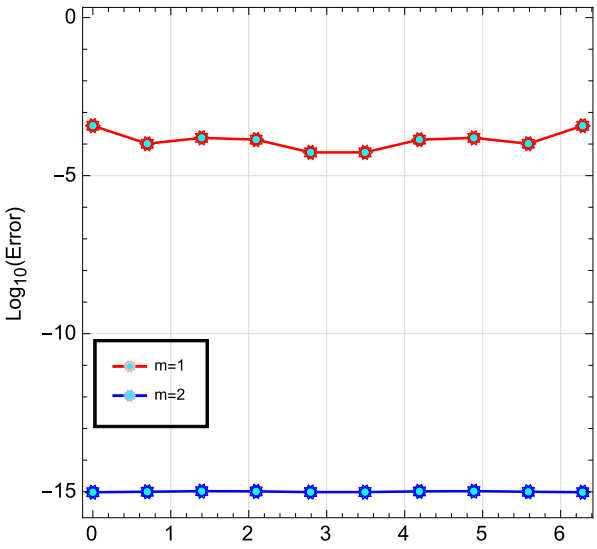

Figure 5. The logarithmic error associated with the proposed method for Example 5.3 with $m = 1, 2$.

This problem has been addressed through the application of the Legendre wavelets method in [18] with $M = 3,\ k = 3, 4, 5$ and the Legendre polynomials method given in [26] with $N = 4, 6, 8$. The comparison of periodic quasi-wavelets using $n = 2,\ m = 1, 2, 3$ with the methods of [18] and [26] are presented in Table 4, which confirms that the periodic quasi-wavelets method in Section 3 gives almost the same solution of the analytic method.

Table 4. Comparison between the periodic quasi-wavelets, the Legendre wavelets, and the Legendre polynomials methods for Example 5.3.

m	periodic quasi-wavelets	k	Legendre wavelets	N	Legendre polynomials
1	3.42×10^{-03}	3	2.43×10^{-02}	4	5.27×10^{-01}
2	1.00×10^{-15}	4	3.77×10^{-03}	6	1.04×10^{-02}
3	0	5	4.96×10^{-04}	8	7.01×10^{-04}

6. Conclusions

A collocation method that employs periodic quasi-wavelets has been introduced to effectively approximate solutions to complex nonlinear Fredholm-Hammerstein integral equations. A thorough examination of the method's convergence, along with numerical results and the uniform error norm, has been conducted. The findings have demonstrated strong agreement with analytical solutions. Notably, adjustable parameters n and m are offered by periodic quasi-wavelets, facilitating more accurate numerical solutions for integral equations. This approach is also easily extendable to general nonlinear Volterra and Fredholm integral equations in the complex plane.

Author contributions

Ahmed Ayad Khudhair: Methodology, Investigation; Saeed Sohrabi: Writing-review & editing, Writing-original draft, Validation, Supervision, Software, Investigation; Hamid Ranjbar: Validation, Formal analysis, Investigation.

Acknowledgments

We express our sincere gratitude to the Editor and the reviewers of this article for their expert assistance and invaluable suggestions, which significantly contributed to the enhancement of the quality of this work.

Conflict of interest

All authors declare no conflicts of interest in this paper.

References

1. M. Asif, I. Khan, N. Haider, Q. Al-Mdallal, Legendre multi-wavelets collocation method for numerical solution of linear and nonlinear integral equations, *Alex. Eng. J.*, **59** (2020), 5099–5109. http://dx.doi.org/10.1016/j.aej.2020.09.040
2. K. Atkinson, A survey of numerical methods for solving nonlinear integral equations, *J. Integral Equ. Appl.*, **4** (1992), 15–47. http://dx.doi.org/10.1216/jiea/1181075664
3. E. Babolian, A. Shahsavaran, Numerical solution of nonlinear Fredholm integral equations of the second kind using Haar wavelets, *J. Comput. Appl. Math.*, **225** (2009), 89–95. http://dx.doi.org/10.1016/j.cam.2008.07.003
4. H. Beiglo, M. Gachpazan, M. Erfanian, Solving nonlinear Fredholm integral equations with PQWs in complex plane, *Int. J. Dyn. Syst. Diffe.*, **11** (2021), 18–30. http://dx.doi.org/10.1504/IJDSDE.2021.113901
5. H. Beiglo, M. Gachpazan, PQWs in complex plane: application to Fredholm integral equations, *Appl. Math. Model.*, **37** (2013), 9077–9085. http://dx.doi.org/10.1016/j.apm.2013.04.018

6. G. Beylkin, R. Coifman, V. Rokhlin, Fast wavelet transform and numerical algorithms I, *Commun. Pur. Appl. Math.*, **44** (1991), 141–183. http://dx.doi.org/10.1002/cpa.3160440202
7. I. Burova, Fredholm integral equation and splines of the fifth order of approximation, *WSEAS Transactions on Mathematics*, **21** (2022), 260–270. http://dx.doi.org/10.37394/23206.2022.21.31
8. H. Chen, Periodic orthonormal quasi-wavelet bases, *Chinese Sci. Bull.*, **41** (1996), 552–554.
9. H. Chen, *Complex harmonic splines, periodic quasi-wavelets: theory and applications*, Dordrecht: Springer, 2000. http://dx.doi.org/10.1007/978-94-011-4251-9
10. H. Chen, S. Peng, A quasi-wavelet algorithm for second kind boundary integral equations, *Adv. Comput. Math.*, **11** (1999), 355–375. http://dx.doi.org/10.1023/A:1018992413504
11. H. Chen, S. Peng, Solving integral equations with logarithmic kernel by using periodic quasi-wavelet, *J. Comput. Math.*, **18** (2000), 487–512.
12. A. Hammerstein, Nichtlineare integralgleichungen nebst anwendungen, *Acta Math.*, **54** (1930), 117–176. http://dx.doi.org/10.1007/BF02547519
13. M. Kamada, K. Toraichi, R. Mori, Periodic spline orthonormal bases, *J. Approx. Theory*, **55** (1988), 27–34. http://dx.doi.org/10.1016/0021-9045(88)90108-6
14. N. Karamollahi, M. Heydari, G. Loghmani, Approximate solution of nonlinear Fredholm integral equations of the second kind using a class of Hermite interpolation polynomials, *Math. Comput. Simulat.*, **187** (2021), 414–432. http://dx.doi.org/10.1016/j.matcom.2021.03.015
15. H. Keller, Geometrically isolated nonisolated solutions and their approximation, *SIAM J. Numer. Anal.*, **18** (1981), 822–838. http://dx.doi.org/10.1137/0718056
16. S. Kumar, A new collocation-type method for Hammerstein integral equations, *Math. Comp.*, **48** (1987), 585–593. http://dx.doi.org/10.1090/S0025-5718-1987-0878692-4
17. M. Lakestani, M. Razzaghi, M. Dehghan, Solution of nonlinear Fredholm-Hammerstein integral equations by using semiorthogonal spline wavelets, *Math. Probl. Eng.*, **1** (2005), 113–121. http://dx.doi.org/10.1155/MPE.2005.113
18. Y. Mahmoudi, Wavelet Galerkin method for numerical solution of nonlinear integral equation, *Appl. Math. Comput.*, **167** (2005), 1119–1129. http://dx.doi.org/10.1016/j.amc.2004.08.004
19. K. Maleknejad, H. Derili, The collocation method for Hammerstein equations by Daubechies wavelets, *Appl. Math. Comput.*, **172** (2006), 846–864. http://dx.doi.org/10.1016/j.amc.2005.02.042
20. K. Maleknejad, M. Hadizadeh, The numerical analysis of Adomian's decomposition method for nonlinear Volterra integral and integro-differential equations, *Int. J. Eng. Sci.*, **8** (1997), 33–48.
21. K. Maleknejad, K. Nedaiasl, Application of Sinc-collocation method for solving a class of nonlinear Fredholm integral equations, *Comput. Math. Appl.*, **62** (2011), 3292–3303. http://dx.doi.org/10.1016/j.camwa.2011.08.045
22. K. Maleknejad, S. Sohrabi, H. Beiglo, PQWs method for Fredholm integral equations with convolution kernel in complex plane, *Proceedings of the* 4^{th} *Iranian Conference on Applied Mathematics*, 2010, 1–7.

23. L. Schumaker, *Spline functions: basic theory*, Cambridge: Cambridge University Press, 2007. http://dx.doi.org/10.1017/CBO9780511618994

24. Z. Shen, Y. Xu, Degenerate kernel schemes by wavelets for nonlinear integral equations on the real line, *Appl. Anal.*, **59** (1995), 163–184. http://dx.doi.org/10.1080/00036819508840397

25. Y. Shi, X. Yang, Z. Zhang, Construction of a new time-space two-grid method and its solution for the generalized Burgers' equation, *Appl. Math. Lett.*, **158** (2024), 109244. http://dx.doi.org/10.1016/j.aml.2024.109244

26. S. Sohrabi, An efficient spectral method for high-order nonlinear integro-differential equations, *U.P.B. Sci. Bull., Series A*, **74** (2012), 75–88.

27. X. Wang, W. Lin, ID-wavelets method for Hammerstein integral equations, *J. Comp. Math.*, **16** (1998), 499–508.

28. A. Wazwaz, *Linear and nonlinear integral equations*, Beijing: Higher Education Press and Berlin: Springer, 2011. http://dx.doi.org/10.1007/978-3-642-21449-3

29. X. Yang, Z. Zhang, Superconvergence analysis of a robust orthogonal Gauss collocation method for 2D fourth-order subdiffusion equations, *J. Sci. Comput.*, **100** (2024), 62. http://dx.doi.org/10.1007/s10915-024-02616-z

30. X. Yang, Z. Zhang, Analysis of a new NFV scheme preserving DMP for two-dimensional sub-diffusion equation on distorted meshes, *J. Sci. Comput.*, **99** (2024), 80. http://dx.doi.org/10.1007/s10915-024-02511-7

AIMS Press

© 2024 the Author(s), licensee AIMS Press. This is an open access article distributed under the terms of the Creative Commons Attribution License (https://creativecommons.org/licenses/by/4.0)